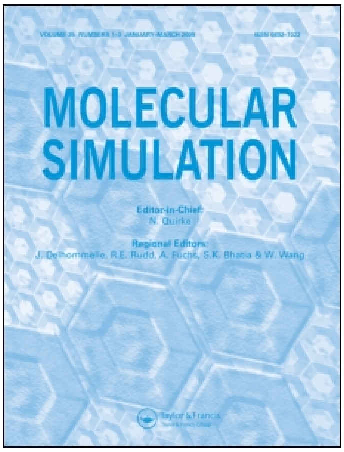

Molecular Simulation
Publication details, including instructions for authors and subscription information:
http://www.informaworld.com/smpp/title~content=t713644482

Non-equilibrium Transport in and on Condensed Matters: Effects of Lattice Vibration and Deterministic Chaos

Dmitry I. Kopelevich[a]; Hsueh-Chia Chang[b]
[a] Department of Chemical Engineering, University of Florida, Gainesville, FL, USA [b] Department of Chemical Engineering, University of Notre Dame, Notre Dame, IN, USA

To cite this Article Kopelevich, Dmitry I. and Chang, Hsueh-Chia(2004) 'Non-equilibrium Transport in and on Condensed Matters: Effects of Lattice Vibration and Deterministic Chaos', Molecular Simulation, 30: 2, 159 — 166

To link to this Article: DOI: 10.1080/0892702031000152127

URL: http://dx.doi.org/10.1080/0892702031000152127

Molecular Simulation, VOL. 30 (2–3), 15 February–15 March 2004, pp. 159–166

Non-equilibrium Transport in and on Condensed Matters: Effects of Lattice Vibration and Deterministic Chaos

DMITRY I. KOPELEVICH[a] and HSUEH-CHIA CHANG[b,*]

[a]*Department of Chemical Engineering, University of Florida, Gainesville, FL 32611, USA;* [b]*Department of Chemical Engineering, University of Notre Dame, Notre Dame, IN 46556, USA*

(Received September 2002; In final form November 2002)

Diffusion of sorbate molecules within a crystal and on the crystal surface can be driven by lattice vibration or by a purely deterministic Hamiltonian mechanism involving coupling between translational degrees of freedom. We delineate these two distinct transport mechanisms for a wide class of sorbate–lattice pairs. When the sorbate–lattice interaction is important, a Langevin model with a spatially non-uniform thermal noise, corresponding to non-homogeneous lattice–sorbate interaction, from our earlier work can be used such that explicit MD simulation of the lattice thermal bath can be circumvented.

Keywords: KAM chaos; Lattice thermal bath; Condensed matter; Non-equilibrium transport

INTRODUCTION

Unlike self-diffusion in the bulk, a sorbate molecule in a crystal or on a crystal surface sees a highly inhomogeneous thermal bath (the crystal lattice) with distinct resonance frequencies. Moreover, the sorbate-bath interaction varies from position to position, thus violating the ergodic approximation in the classical diffusion theory. In fact, whether such transport can be described as diffusion, with a transient variance that grows linearly with time, is unclear. It is reasonable to expect that a quasi-equilibrium theory, like the classical transition state theory (TST), would not be able to capture the effect of this inhomogeneous and non-white stochastic forcing by the lattice. However, explicit molecular dynamics (MD) simulation of the lattice dynamics to capture the lattice thermal bath remains expensive. It would be highly desirable to derive a Langevin equation for the sorbate, with the lattice stochastic forcing represented by a spatially inhomogeneous and non-white thermostating strategy.

In an earlier publication [1,2], we have exploited the separation of timescales between the sorbate transport time and the inverse lattice vibration frequency to derive such a Langevin equation. In this presentation, we use this formulation to examine another peculiar sorbate transport mechanism in and on condensed matters: deterministic sorbate transport in a multi-dimensional potential without lattice vibration or any other stochastic thermal noise. As shown in our earlier exposition [3], such deterministic transport of a lone sorbate occurs because of KAM chaos. When the sorbate inertia is high and the sorbate is hence never near equilibrium, its different translational degrees of freedom can couple to produce chaotic sorbate trajectories in the phase space. At strong coupling, the probability of finding the particle at any location within a potential minimum is uniform (ergodic) and its probability of jumping to the nearby sites resembles that of a random walk. Yet if the sorbate is represented by a single point mass, this seemingly random sorbate dynamic is described by three deterministic Hamiltonian degrees of freedom (six ODE's) without any stochastic forcing.

Since inertia is important for this deterministic chaos, the sorbate particle tends to "rattle" within each potential minimum and can undergo multi-site ballistic hops. Indeed, both phenomena have been observed in recent MD simulations

---

*Corresponding author. E-mail: hsueh-chia.chang.2@nd.edu

ISSN 0892-7022 print/ISSN 1029-0435 online © 2004 Taylor & Francis Ltd
DOI: 10.1080/0892702031000152127

(with and without lattice vibration) and experiments. Recent field ion microscopy studies [4–6] of W and Pd adatoms on W(211) and Ir clusters on Ir(111), scanning tunneling microscopy studies [7] of Ag clusters on Ag(100), and related MD simulations [8,9] show exactly these behaviors. Most intriguingly, even though multi-site ballistic flights are expected to be non-diffusive, MD simulations show that they remain diffusive but with a diffusive length that is several times the lattice unit-cell length.

Multi-site hops, however, can still occur if the transport is stochastically driven by sorbate–lattice interaction, but with a (low-noise) weak stochastic forcing. This noise-driven transport also has high inertia and is distinctly non-equilibrium. It is hence important, for a fundamental understanding of the transport mechanisms and for MD simulation strategies, to determine when stochastic noise can be truly neglected and the transport is purely deterministic. We expect, for example, the transport rate as a function of temperature to be different for low-noise stochastic transport and purely deterministic transport.

In this paper, we examine a model multi-dimensional surface potential to determine the classification criteria for weak and strong noise transport due to stochastic forcing by lattice vibration and for noise-free transport by deterministic chaos. We then apply these criteria to our earlier Langevin model [1] to examine the importance of lattice vibration in a large family of lattice–sorbate pairs. A small subset of such systems are found to be unaffected by lattice vibration and undergo transport by the deterministic mechanism. Others thought earlier to be unaffected by lattice vibration are found to be stochastically driven though with a low-noise mechanism.

CLASSICAL ONE-DIMENSIONAL MECHANISMS

The classical transition state theory considers escape of a sorbate from a one-dimensional potential well. TST assumes that the sorbate spends enough time inside a potential well to equilibrate with thermal bath. TST further assumes that the transport of sorbate from one potential well to another occurs via a fast jump so that the interaction between the sorbate and the thermal bath during this jump can be neglected. Under these equilibrium assumptions, the escape rate k_{TST} of the particle is given by the Boltzmann-averaged flux across the potential barrier,

$$k_{\mathrm{TST}} = \frac{\omega}{2\pi} e^{-\Delta\Phi/k_{\mathrm{B}}T}, \tag{1}$$

where $\Delta\Phi$ is the height of the potential barrier, ω is the frequency of vibration of the sorbate inside the potential well, k_{B} is the Boltzmann constant, and T is the temperature. Note that the TST rate expression (1) does not account for the strength of coupling between the sorbate and thermal bath. This reflects the assumptions of TST that, although thermal interactions drive the sorbate motion, the details of the thermal bath can be neglected. TST was significantly improved by Kramers [10] who considered one-dimensional sorbate motion and assumed that it is described by the Langevin equation, which allows one to explicitly account for the details of the interaction between sorbate and thermal bath,

$$M\ddot{x} = -\nabla\Phi(x) - \gamma\dot{x} + F(t), \tag{2}$$

where M and x are the sorbate mass and position, respectively, and $\Phi(x)$ is the potential energy of interaction between sorbate and rigid lattice. Effects of lattice vibration on the sorbate motion are captured by the friction term $\gamma\dot{x}$ and the random force $F(t)$, which are related by the fluctuation-dissipation theorem,

$$\langle F(t)F(s)\rangle = 2k_{\mathrm{B}}T\delta(t-s). \tag{3}$$

The Langevin equation possesses two timescales: the thermalization timescale $\tau_{\mathrm{therm}} = 1/\gamma$ and the timescale of ballistic motion of the sorbate $\tau_{\mathrm{ballist}} = 1/\omega$. The ratio of these two timescales, $\nu = \gamma/\omega$, is one of the two key parameters of the system. The other key parameter is the normalized height of the potential barrier, $\Delta\Phi/k_{\mathrm{B}}T$. Depending on the values of these parameters, the sorbate undergoes one of the following two qualitatively different diffusion regimes.

If the thermal coupling is strong or the potential well is very deep, i.e. if

$$\nu \geq 1 \quad \text{or} \quad \nu \gg k_{\mathrm{B}}T/\Delta\Phi, \tag{4}$$

then the sorbate is always at equilibrium with the thermal bath and hence the sorbate inertia can be neglected. In this equilibrium diffusion regime, the transport rate has the classical Arrhenius temperature dependence and is given by the following expression:

$$k = k_{\mathrm{TST}}\left(\sqrt{(\nu/2)^2 + 1} - \nu/2\right). \tag{5}$$

Note that the transition-state theory result (1) holds only if

$$k_{\mathrm{B}}T/\Delta\Phi \ll \nu \ll 1. \tag{6}$$

In other words, in the TST limit the noise is weak, thus ensuring that the thermal interactions during the jump of the sorbate over the potential barrier are negligible. However, since the potential barrier is very high, the particle spends enough time inside the potential well to equilibrate with the thermal bath.

Note that the lattice–sorbate interaction parameter is negligible only in the TST limit. If the condition (6) does not hold, one has to modify the pre-exponential factor to account for the effects of lattice vibration.

When neither of the conditions (4) hold, the other diffusion mechanism, non-equilibrium low-noise diffusion takes place. In this case, sorbate inertia becomes important and significant ringing occurs within the potential well. In the low-noise diffusion regime, the energy of the sorbate is not at equilibrium but is a slowly changing quantity. The diffusion takes place in two stages. First, the sorbate oscillates back and forth inside the potential well, closely following constant energy orbits and slowly moving from one orbit to another. After the sorbate has gained enough energy to cross the separatrix, it undergoes a convective transport along the separatrix until it thermalizes in another potential well. Kramers [10] obtained the following escape rate from a potential well in the low-noise diffusion regime:

$$k = \frac{\gamma S}{k_{\mathrm{B}}T}\frac{\omega}{2\pi}e^{-\Delta\Phi/k_{\mathrm{B}}T}. \tag{7}$$

Here, S is the value of the action of the particle at the separatrix. Note that the expression (7) has a temperature-dependent pre-exponential factor and hence the diffusion in the low noise regime does not obey the Arrhenius law. Note also the importance of resolving the specific sorbate–lattice interaction parameter γ for this non-equilibrium regime. In the limit when there is negligible interaction with the lattice ($\gamma = 0$), it predicts zero transport rate in a one-dimensional potential.

The results cited above were obtained for a potential energy with only one potential well, i.e. it is assumed that the particle never comes back after it crossed over the potential barrier. However, surface and intracrystalline diffusion takes place in a periodic potential and hence one has to modify Kramers' theory in order to study diffusion in such systems. This modification is relatively straightforward in the high-noise regime, since the transport process can be readily decomposed into uncorrelated jumps (described by Kramers) from one potential well to another. However, the situation is more complicated in the low-noise regime. Instead of uncorrelated jumps, the transport occurs along the separatrix of the $x - v$ phase space. In particular, the sorbate does not have to thermalize in the nearest potential well, but can make the long jumps referred to earlier.

DETERMINISTIC DIFFUSION IN MULTI-DIMENSIONS

However, these classical mechanisms are strictly applicable only to one-dimensional potential wells. In an earlier paper [3], we found a new transport mechanism in realistic multi-dimensional potentials that can occur even without noise (lattice–sorbate interaction, $\gamma = 0$).

In order to gain better understanding of the interplay between deterministic chaos and thermal noise-driven diffusion, we performed MD simulations of surface sorbate motion in three-dimensional space. The thermal noise was assumed to be white and hence the Langevin equation

$$M\ddot{\mathbf{x}} + \gamma\dot{\mathbf{x}} = -\nabla\Phi(\mathbf{x}) + \mathbf{F}(t),$$

$$\langle F_i(t)F_j(s)\rangle = 2k_{\mathrm{B}}T\gamma\delta(t-s)\delta_{ij}, \quad i,j = 1,2,3, \tag{8}$$

was simulated. The friction coefficient γ was assumed to be homogeneous and its value was artificially varied over several orders of magnitude.

To analyze the interaction between chaotic and thermal driving forces for diffusion, the following model of potential energy of interaction between an adsorbate atom and a rigid crystal lattice was chosen:

$$\begin{aligned}\Phi(x,y,z) = {} & E_0 + (E_0 - E_1 f(x,y)) \\ & \times\Big\{\exp\left[-2(\alpha_0 + a_1 f(x,y))(z - z_0 f(x,y))\right] \\ & -2\exp\left[-(\alpha_0 + \alpha_1 f(x,y))(z - z_0 f(x,y))\right]\Big\},\end{aligned} \tag{9}$$

where

$$f(x,y) = \cos\big(2\pi x/a) + \cos(2\pi(y - a/2)/a\big). \tag{10}$$

The values of the model parameters are summarized in Table I. These values, as well as the results reported in this and the following sections, are in terms of characteristic units which are summarized in Table II.

This model potential was proposed by Zhang and Metiu [8] and it mimics interaction between hydrogen adatom and a (100) surface of Cu. The crystal surface is parallel to the *Oxy* plane and the z-axis is perpendicular to the surface and points towards the vacuum. For fixed values of x and y, the function $\Phi(x,y,z)$ is the Morse potential; also, the potential is periodic in the x and y directions with period $a = 1$. The minima of the potential are located at point $x = (0.5, 0.0, -2.818)$ and its periodic images,

TABLE I Parameters of the potential model

Model parameter	*Value (in terms of characteristic units)*
E_0	2.4707
E_1	0.5
α_0	2.9939
α_1	0.4947
A	1.0
z_0	0.1409

TABLE II Definitions and values of characteristic units

Quantity	*Characteristic value*	*Definition*
Length	$l_c = a = 2.62\,\text{Å}$	Shortest distance between two surface atoms
Mass	$m_c = 1.6726231 \times 10^{-27}\,\text{kg}$	Mass of hydrogen atom
Energy	$E_c = 0.5022\,\text{eV}$	Barrier height for diffusion of H on Cu
Time	$t_c = 2.671 \times 10^{-14}$	$l_c\sqrt{m_c/E_c}$
Diffusivity	$D_c = 1.285 \times 10^{-6}$	l_c^2/t_c

and the saddle points are located at point $x = (0, 0, 0)$ and its periodic images. Note that the additive constant in Eq. (9) has been chosen so that the potential energy of the sorbate at the saddle point is zero.

When the thermal noise is absent, the Langevin equation (8) reduces to the Newton equation for deterministic motion,

$$M\ddot{\mathbf{x}} = -\nabla\Phi(\mathbf{x}). \tag{11}$$

The simulations of this equation were performed using the velocity Verlet algorithm with the step size in time $\Delta t = 10^{-3}$. This choice of the algorithm and the step size yields good conservation of the total energy of the sorbate: in all simulations performed, energy fluctuation due to numerical errors was less than 0.2% of the height of the potential barrier.

Typical trajectories obtained from the constant-energy simulations are shown in Fig. 1. As is evident, these trajectories are rather chaotic. The sorbate transfers its energy from one degree of freedom to another to overcome a potential barrier. At lower values of energy E, the sorbate spends a long time inside each potential well, since it takes more time for it to transfer its energy into the degrees of freedom relevant to the transport across the potential barrier. For larger values of energy E, on the other hand, the sorbate is easily transported from one unit cell to another and long jumps are the major transport mode in this case. Such long jumps resemble those driven by low noise diffusion in a one-dimensional potential but will be shown to have a completely different rate. In order to quantify the observed chaoticity of trajectories, the velocity autocorrelation functions for horizontal and vertical velocities,

$$C_{\alpha\alpha}(E,\tau) = \frac{\langle v_\alpha(\tau)v_\alpha(0)\rangle}{\langle v_\alpha^2(0)\rangle}, \quad \alpha = x, y, z, \tag{12}$$

were computed. Here, v_α is the α Cartesian component of the sorbate velocity and the angular brackets denote microcanonical ensemble averaging. To compute the ensemble average, a large number N_{sample} of sample sorbate trajectories with fixed energy E was simulated. Initial conditions for each of these trajectories were taken from a uniform distribution on a constant-energy surface. The initial sorbate position $x(0)$ was assumed to be uniformly distributed in the rectangle $[0,1] \times [0,1] \times [-0.5, 0]$ and the initial sorbate velocity was uniformly distributed on the sphere with radius $\sqrt{2(E - \Phi(x(0))/M}$. The number N_{sample} of simulated trajectories was chosen to be 40,000. An estimated error of statistical averaging for this ensemble is within 10%.

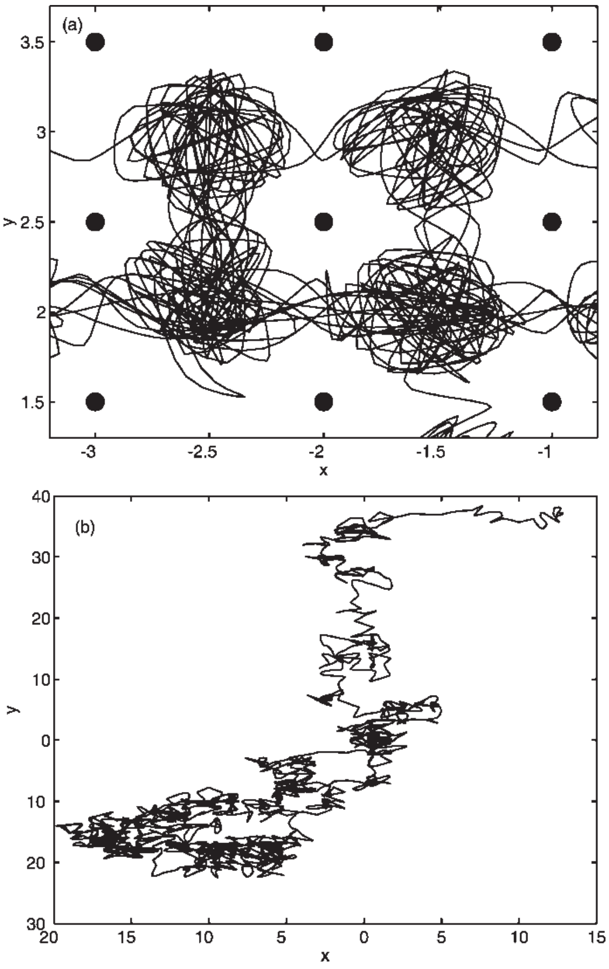

FIGURE 1 Examples of simulated trajectories in the absence of thermal noise: (a) a trajectory at $E = 0.5$ (locations of the surface atoms are indicated by solid circles); (b) a trajectory at $E = 2.0$. Note the difference in length scales.

The symmetry of the model potential (9) with respect to interchange of x- and y-directions suggests that the autocorrelation functions in the x- and y-direction should coincide if the motion of the sorbate is ergodic. This is indeed true, and the computed discrepancy between C_{xx} and C_{yy} for the same value of E is smaller than the statistical error. The autocorrelation functions C_{xx} and C_{zz} for several values of the sorbate energy are shown in Fig. 2. The observed decay of autocorrelation functions indicates that motion of the sorbate is uncorrelated with its history of motion on the timescale of about 10 time units. That is, the sorbate loses its memory and explores the phase space. This result gives another indication of the ergodicity of the sorbate motion.

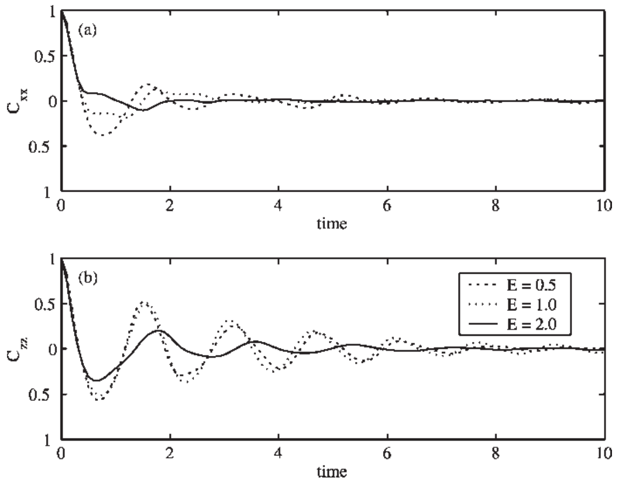

FIGURE 2 (a) Horizontal and (b) vertical velocity autocorrelation functions for simulations with sorbate energy $E = 0.5$, $E = 1.0$, and E = 2.0.

In order to confirm the ergodicity, the autocorrelation functions $C_{\alpha\alpha}$ are computed using the definition (12) with the ensemble averaging replaced by the time averaging:

$$C_{\alpha\alpha}(\tau) = \frac{\int_0^\infty v_\alpha(\tau+\tau_0)v_\alpha(\tau)\mathrm{d}\tau_0}{\int_0^\infty v_0^2(\tau_0)\mathrm{d}\tau_0}. \tag{13}$$

To compute the time average, one long simulation (up to time $t = 10^4$) for a fixed sorbate energy E was performed and then the convolution integral in the numerator of Eq. (13) was computed using the fast Fourier transform method. The autocorrelation functions computed using the ensemble averaging of Eq. (12) and the time averaging of Eq. (13) are found to be essentially identical. This proves the ergodicity of the system, i.e. that the time average coincides with the ensemble average.

Since the velocity autocorrelation functions vanish at large enough time, the Green-Kubo formula implies that the sorbate motion is diffusive, i.e. the variance $\langle x^2(t) + y^2(t)\rangle$ of horizontal sorbate coordinates scales linearly with time t. This is also confirmed by a direct calculation of $\langle x^2(t) + y^2(t)\rangle$ and results of this calculation are presented in Fig. 3. The transport process from one minimum to the next is hence a process with a well-defined diffusivity, even though there is only one sorbate and stochastic thermal noise is absent. The ensemble averaging $\langle x^2(t) + y^2(t)\rangle$ was performed over the large number of simulated trajectories with initial conditions for each trajectory chosen from the uniform distribution on the constant energy surface. The number of simulated trajectories was chosen so that the relative error in the estimated diffusion coefficient was less then 5%. The diffusion coefficient D was obtained by the least squares fit to the Einstein formula

$$\frac{\langle x^2(t) + y^2(t)\rangle}{4} = Dt. \tag{14}$$

Thus obtained deterministic diffusivity $D(E)$ is shown in Fig. 4a and is seen to increase monotonically with energy. Moreover, it is observed that the timescale of the sorbate transport over one unit cell is of the same order of magnitude as the correlation time of the sorbate velocity. Assuming that the neglected thermalization will slowly equilibrate the sorbate, the long-time deterministic diffusivity $D(T)$ for a given temperature T is obtained

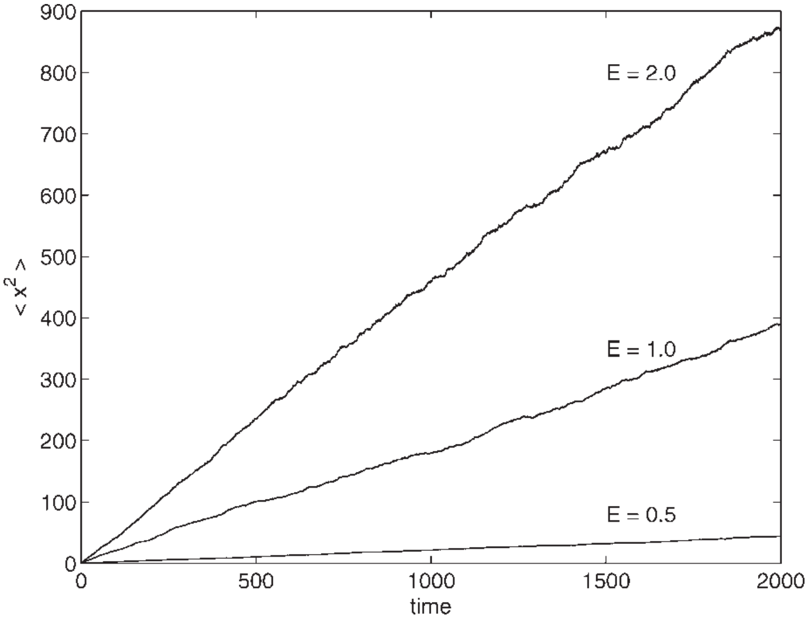

FIGURE 3 Variance $\langle x^2(t) + y^2(t)\rangle$ of sorbate position as a function of time for $E = 0.5$, $E = 1.0$, and E = 2.0.

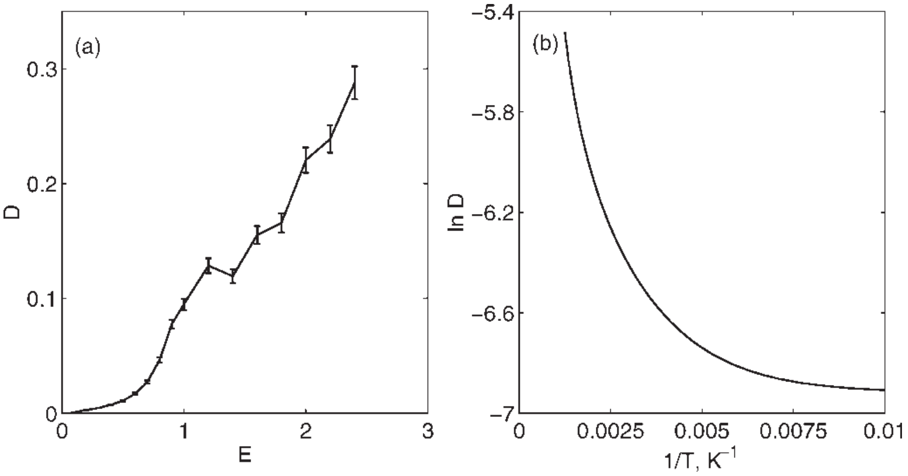

FIGURE 4 Deterministic diffusivity of H on Cu(001) surface: (a) diffusivities for different energies; (b) Arrhenius plot of dependence of deterministic diffusivity on temperature; $D(T)$ is obtained by the Boltzmann averaging.

by performing the Boltzmann averaging over the constant-energy diffusivities $D(E)$,

$$D(T) = \frac{\int D(E) e^{-E/k_B T}\, dE}{\int e^{-E/k_B T}\, dE}. \tag{15}$$

Temperature dependence of this diffusivity deviates from the Arrhenius law, as is seen in Fig. 4b.

EFFECT OF THERMAL NOISE

The thermal bath effect can now be modeled by the Langevin equation (8). With this model, relative importance of deterministic and noise-driven diffusion mechanism can be captured by the ratio of the thermalization timescale τ_{therm} and the transport timescale τ_{transp}.

The thermalization timescale τ_{therm} is inversely proportional to the sorbate-thermal bath coupling γ. The transport timescale τ_{therm} is inversely proportional to the transport rate k and depends on a particular transport mechanism. For the diffusion driven by high noise, k has been described in the "Classical One-dimensional Mechanisms" Section. For the low-noise and deterministic transport mechanisms, k depends on a specific geometry. In the previous section, the transport rate has been obtained for an example of deterministic surface diffusion.

The Langevin equation (8) has been simulated using a generalization of the velocity Verlet algorithm,

$$\mathbf{x}(t_{n+1}) = \mathbf{x}(t_n) + b_1 \mathbf{v}(t_n) - \frac{\Delta t}{2M} b_1 \nabla \Phi(\mathbf{x}(t_n)) + \frac{1}{M}\mathbf{R}_n^{(1)}, \tag{16}$$

$$\mathbf{v}(t_{n+1}) = b_0 \mathbf{v}(t_n) - \frac{\Delta t}{2M}\left[\nabla \Phi(\mathbf{x}(t_{n+1})) + \nabla \Phi(\mathbf{x}(t_n)) b_0\right] + \frac{1}{M}\mathbf{R}_n^{(2)}, \tag{17}$$

where $\mathbf{R}_n^{(1)}$ and $\mathbf{R}_n^{(2)}$ are random vectors with Gaussian distribution, zero mean, and the following covariance matrix:

$$\left\langle \mathbf{R}_n^{(i)} \mathbf{R}_m^{(j)} \right\rangle = 2k_B T \gamma \mathbf{I} \delta_{mn} C_{ij}, \quad i,j = 1,2. \tag{18}$$

Here, $\mathbf{I}$ is a 3×3 unit matrix and

$$C_{11} = (\Delta t - 2b_1 + b_2)/\gamma^2, \tag{19}$$

$$C_{12} = C_{21} = (b_1 - b_2)/\gamma, \tag{20}$$

$$C_{22} = b_2. \tag{21}$$

Finally,

$$b_0 = e^{-\gamma \Delta t},\ b_1 = \frac{1 - b_0}{\gamma},\ b_2 = \frac{1 - b_0^2}{2\gamma},\ t_n = n\Delta t, \tag{22}$$

and the stepsize

$$\Delta t = \min\left(\frac{10^{-2}}{\gamma}, 10^{-3}\right) \tag{23}$$

has been chosen to be inversely proportional to γ so that smaller stepsize is used to numerically resolve Brownian motion due to stronger thermal noise.

Results of the simulations are shown in Fig. 5. When τ_{therm} is much larger than the average residence time τ_{transp}, i.e. when $\gamma \to 0$, the diffusivity does not vanish like it did in the one-dimensional case predicted by Eq. (7), but approaches the value of the deterministic diffusivity. In fact, the deterministic value is approached for γ as large as unity. This implies that, when it is not excessively large, the one-dimensional theory (7) is invalid and transport is

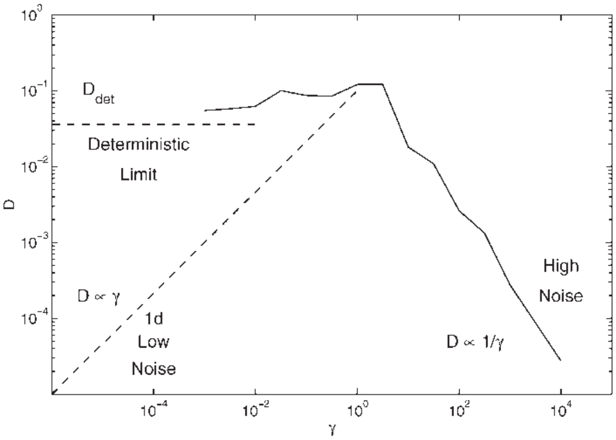

FIGURE 5 Results of simulations of the Langevin equation (8) with the model potential (9) at a fixed temperature. Diffusivity is obtained for different values of the coupling parameter γ and is shown by the solid line. At small γ, the diffusivity approaches the deterministic value D_{det}, which is shown by a dashed line. The one-dimensional result for diffusivity in the low-noise regime is also shown by a dashed line.

dominated by the deterministic mechanism at $\gamma = 0$. For large values of γ, however, the diffusivity deviates significantly from the deterministic value and scales as $1/\gamma$ similarly to the one-dimensional case. Moreover, a shallow maximum occurs near $\gamma = 1$ where the two regimes overlap. As a general rule, deterministic diffusion is larger than high-noise thermal diffusion by as much as two orders of magnitude. Multi-site jumps are common in deterministic diffusion but their rates cannot be captured by the one-dimensional low-noise theory (7), which also predicts long jumps.

Hence, depending on the value of coupling between the sorbate motion and the thermal noise, the diffusion can be driven by different mechanisms. In particular, a new deterministic mechanism that dominates for intermediate and weak sorbate-bath coupling was described. These results can be summarized in a phase diagram for multidimensional diffusion shown in Fig. 6, where conditions (4) have also been included.

The deterministic diffusion is dominant when

$$\tau_{\text{therm}} \gg \tau_{\text{transp}}, \tag{24}$$

where $\tau_{\text{therm}} \propto 1/\gamma$ and, for a given temperature T, the timescale of the sorbate transport $\tau_{\text{transp}}(T)$ was obtained from the Boltzmann averaging of the transport timescale $\tau_{\text{transp}}(E)$ at the fixed energy E,

$$\tau_{\text{transp}}(T) = \frac{\int \tau_{\text{transp}}(E) e^{-E/k_{\text{B}}T}\, \mathrm{d}E}{\int e^{-E/k_{\text{B}}T}\, \mathrm{d}E}. \tag{25}$$

The value of $\tau_{\text{transp}}(E)$ depends on the specific system, and in general, should be computed numerically.

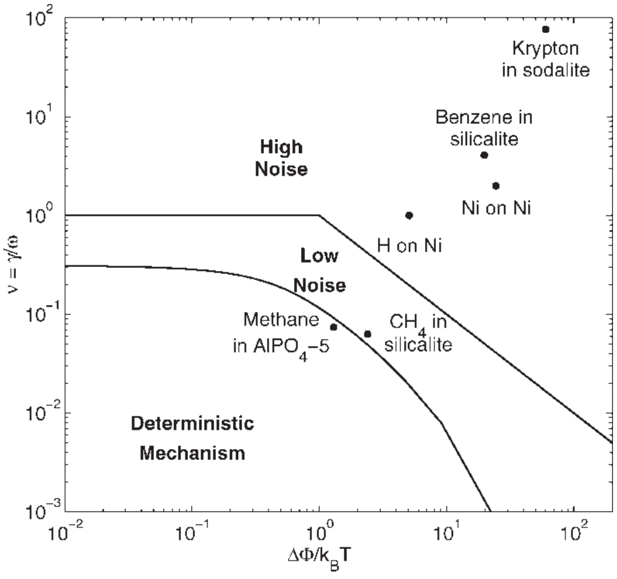

FIGURE 6 Phase diagram with several sorbate–lattice systems placed on it according to the values of the dimensionless friction ν and the temperature-normalized potential barrier $\Delta\Phi/k_{\text{B}}T$ (at room temperature).

CLASSIFICATION AND SIMULATION STRATEGIES

It is clear from the previous two sections that non-equilibrium deterministic transport in a multi-dimensional potential can be Markovian with little memory. It can also exhibit ballistic multi-site hops. These features resemble diffusive transport driven by weak stochastic forcing. However, as seen in Fig. 5, the quantitative dependence on the dissipation parameter γ and hence on temperature are distinctly different for the deterministic mechanism and the low-noise mechanism. It is, in fact, the dominant mechanism with low and intermediate noise.

The Langevin equation (8) assumes a spatially homogeneous noise with a zero correlation time. A more realistic model that accounts for the band gaps in the lattice vibration spectra (hence finite correlation time for noise) and spatial inhomogeneity in the sorbate–lattice interaction is based on the generalized Langevin equation for the sorbate motion [1,11,12],

$$M\ddot{\mathbf{x}} = -\nabla \Phi_{\text{eff}}(\mathbf{x}) - \int_0^t \eta(\mathbf{x}(t), \mathbf{x}(s), t-s)\dot{\mathbf{x}}(s)\mathrm{d}s + \mathbf{F}(\mathbf{x}(t), t). \tag{26}$$

Here, $\Phi_{\text{eff}}(\mathbf{x})$ is the effective sorbate–lattice interaction potential energy, which accounts for mean-field effects of lattice vibration, $\eta(\mathbf{x}(t), \mathbf{x}(s), t-s)$ is the memory friction kernel, and $\mathbf{F}(t)$ is the stochastic force, which has a Gaussian distribution with zero mean and is related to the friction kernel η by the fluctuation-dissipation theorem,

$$\langle \mathbf{F}(t) \rangle = 0, \quad \langle \mathbf{F}(t)\mathbf{F}(s) \rangle = k_B T \eta(\mathbf{x}(t), \mathbf{x}(s), t - s). \quad (27)$$

Despite the complicated position- and time-dependence of the parameters of the generalized Langevin equation (26), we have shown [1] that one can extract representative potential barriers $\Delta\Phi$ and harmonic frequency ω from the maxima and minima of a particular sorbate/lattice pair. A representative dissipation parameter γ can be obtained from a spatial average over the unit cell with a Boltzmann weight. Alternatively, the value at the transition state can be taken.

The results shown in Fig. 6 are for sorbate diffusion in zeolites and for surface diffusion on metal. As is evident, methane undergoes purely deterministic transport in zeolites $AlPO_4$-5 and silicalite. This resolves a controversy regarding the methane-silicalite pair that is detailed in our earlier publication. [3] Literature simulations [13,14] of this system that include lattice dynamics and with a rigid lattice were found to produce the same diffusivity that agrees with measured data over a 200 degrees K range. The deterministic mechanism clearly dominates here and the lattice vibration does not contribute to sorbate transport. MD simulations with a rigid lattice can produce accurate results. However, such simulations should be done at constant energy and without thermostating. Boltzmann average of the transport rate as in Eq. (25) should then be done for the ensemble of simulations.

For extremely high-noise and near-equilibrium transport, diffusion rates can be captured with a multidimensional generalization of the classical one-dimensional theory (5). Since the sorbate dynamics inside the potential well do not affect the near-equilibrium diffusion rate, thermal bath needs to be resolved only at the potential barrier. For example, near-equilibrium stretching of zeolite cages can be important and this should be captured with a TST type theory that allows for the stretching of lattice bonds near the sorbate. This was done in our TST theory presented in [2] for inert gases in sodalite. Simple barrier height calculation, with allowance for cage bond stretching, was found to provide accurate estimate to the transport rate.

Hence, the anisotropy and correlated features of stochastic lattice forcing are only important for moderately high noise transport. Surface transport like H and Ni on Ni fall in this category. In fact, the surface diffusion of H on Ni, thought to be deterministic and simulated with a rigid lattice [8], actually suffers from considerable stochastic forcing. MD simulation of its dynamics must include lattice vibration. This can be done by simulating the lattice explicitly or by using the generalized Langevin equation which captures lattice vibration with a non-homogeneous stochastic noise and a finite correlation time. The latter strategy is obviously more convenient if a simulation package for colored noise is available.

A related transport problem is Knudsen transport of gas molecules in a pore whose pore size is smaller than the mean free path. These nanopores are bigger than the zeolite pores considered here. Hence lattice–sorbate interaction is only important when ballistic gas molecules collide with the pore walls. A companion paper [15] in this proceeding will show that whether the collision is elastic and specular is determined by a deterministic diffusive mechanism on the pore wall.

References

[1] Kopelevich, D.I. and Chang, H.-C. (2001) "Does lattice vibration drive diffusion in zeolites?", *J. Chem. Phys.* **114**, 3776.

[2] Kopelevich, D.I. and Chang, H.-C. (2001) "Diffusion of inert gases in silica sodalite: importance of lattice flexibility", *J. Chem. Phys.* **115**, 9519.

[3] Kopelevich, D.I. and Chang, H.-C. (1999) "Nonequilibrium-diffusion in zeolites due to deterministic Hamiltonian Chaos", *Phys. Rev. Lett.* **83**, 1590.

[4] Senft, D.C. and Ehrlich, G. (1995) "Long jumps in surface diffusion: one-dimensional migration of isolated adatoms", *Phys. Rev. Lett.* **74**, 294.

[5] Wang, S.C. and Ehrlich, G. (1997) "Diffusion of large surface clusters: direct observations on Ir(111)", *Phys. Rev. Lett.* **79**, 4234.

[6] Wang, S.C., Kürpick, U. and Ehrlich, G. (1998) "Surface diffusion of compact and other clusters: Ir_x on Ir(111)", *Phys. Rev. Lett.* **81**, 4923.

[7] Wen, J.-M., Chang, S.-L., Burnett, J.W., Evans, J.W. and Thiel, P.A. (1994) "Diffusion of large two-dimensional Ag clusters on Ag(100)", *Phys. Rev. Lett.* **73**, 2591.

[8] Zhang, Z. and Metiu, H. (1990) "Adsorbate migration on solid surface—the connection between hopping dynamics and the atom-surface interaction energy", *J. Chem. Phys.* **93**, 2087.

[9] Luedtke, W.D. and Landman, U. (1999) "Slip diffusion and Lévy flights of an adsorbed gold nanocluster", *Phys. Rev. Lett.* **82**, 3835.

[10] Kramers, H.A. (1940) "Brownian motion in a field of force and the diffusion model of chemical reactions", *Physica* **7**, 284.

[11] Zwanzig, R. (1973) "Nonlinear generalized Langevin equations", *J. Stat. Phys.* **9**, 215.

[12] Tsekov, R. and Ruckenstein, E. (1994) "Stochastic dynamics of a subsystem interacting with a solid body with application to diffusive processes in solids", *J. Chem. Phys.* **100**, 1450.

[13] Demontis, P., Suffritti, G.B. and Mura, P. (1992) "A molecular dynamics study of diffusion of methane in silicalite molecular sieve at high dilution", *Chem. Phys. Lett.* **191**, 553.

[14] June, R.L., Bell, A.T. and Theodorou, D.N. (1990) "Molecular dynamics study of methane and xenon in silicalite", *J. Phys. Chem.* **94**, 8232.

[15] Arya, G., Chang, H.-C. and Maginn, E.J. (2003) "Molecular simulation of Knudsen wall-slip in micro-channels: effect of wall morphology,", *Mol. Sim.* **29**, 697.